THE VERIFICATION OF RADON PROTECTIVE MEASURES BY MEANS OF A COMPUTER MODEL

Martin Jiranek & Zbynek Svoboda

Czech Technical University in Prague
Faculty of Civil Engineering
166 29 Prague 6 - Czech Republic

ABSTRACT

The numerical model for verification of various radon protective measures has been developed. This model is based on the partial differencial equation for the two-dimensional steady-state radon transport caused by diffusion and convection. The finite element method was used to obtain the numerical solution of the governing equation. The general finite element formulation was derived by means of the Petrov-Galerkin method with weighting functions different from interpolation functions.

The performance of soil ventilation systems has been studied with this model. The results of simulation demonstrate that the soil depressurization systems are effective in the majority of cases while the soil pressurization systems only in case of permeable soils.

INTRODUCTION

Radon protective measures are designed to reduce the radon flow from the ground or from the building materials into a building interior. The improvement of the efficiency of these measures is very important for the minimizing of the health risk caused by radon.

The verification of most radon protective measures can be realized by means of a computer model based on the partial differencial equation for the two-dimensional steady-state radon transport in a porous medium. This equation can be expressed as

$$D_e \nabla^2 C + \frac{k}{\varepsilon \eta} \vec{\nabla} p . \vec{\nabla} C + G - \lambda C = 0 \qquad (1).$$

The first term on the left-hand side of the equation (1) represents the radon transport due to diffusion, the second term represents the radon transport due to convection. The third term expresses the increase of radon concentration due to radon generation rate in the soil or material pores and the last term represents the drop in radon concentration due to radioactive decay.

The assumptions made in the model are as follows:

- each element is homogeneous, (i.e. permeability, porosity and radon diffusion coefficient are constant within each element),
- soil gas is incompressible,
- flow of soil gas is linear according to Darcy´s Law

$$\vec{v} = -\frac{k}{\eta} \vec{\nabla} p \qquad (2)$$

- pressure distribution is governed by Laplace equation

$$\nabla^2 p = 0 \qquad (3).$$

ANALYSIS

The equation (1) belongs to the convective-diffusion equations family. The numerical solution of any type of convective-diffusion equation is more complicated than the numerical solution of related diffusion equation. The main reason is the convective transport term which can, under certain conditions, introduce instabilities and inaccuracies in the solution not present in the diffusion equation.

The finite element method was used for the solution of the equation (1). The general finite element formulation of the governing equation (1) was derived by means of the Petrov-Galerkin method. This approach which is also known as streamline balancing diffusion or streamline Petrov-Galerkin process is based on the special selection of the weighting functions different from the interpolation functions.

The identity of the weighting and interpolation functions is characteristic for the standard Galerkin method which is the most commonly used method in the finite element solution of the field problems. Unfortunately this method can not be applied to the equation (1), because it leads to the numerical

oscillations mentioned above, as was already shown by several researchers (Zienkiewicz, Huebner).

As the Petrov-Galerkin method is one of the weighted residuals methods, the derivation of the finite element formulation starts with equation

$$\int_{\Omega^{(e)}} \left[D_e \nabla^2 C - \frac{\vec{v}}{\varepsilon} \vec{\nabla} C + G - \lambda C \right] W_i \, \mathrm{d}\,\Omega = 0 \quad (4)$$

which expresses the requirement that the residual or error obtained by substitution of the approximation into the equation (1) must be orthogonal to the weighting functions W_i.

The approximation of the unknown function C is taken as

$$C = N_i^{\,T} C_i \qquad (5).$$

The interpolation functions N_i are chosen in accordance with the type of the finite elements.

The definition of the weighting functions is very important in this case. The approach recommended by Zienkiewicz takes the weighting functions as

$$W_j = N_j + \frac{\omega h}{2} \frac{u \frac{\partial N_j}{\partial x} + v \frac{\partial N_j}{\partial y}}{|u|} \qquad (6).$$

If the value of ω is chosen as

$$\omega = \coth Pe - \frac{1}{Pe} \qquad (7)$$

with Peclet number defined as

$$Pe = \frac{|u| h}{2 \varepsilon D_e} \qquad (8)$$

then according to Zienkiewicz exact nodal values will be given for all values of *Pe*, i.e. the numerical oscillations do not arise for any possible rate between convective transport and diffusive transport. It can be clearly seen that the weighting functions are different from zero only in the direction of the velocity vector.

The equation (5) can be substitued into the equation (4). The integration by parts can be then applied to the first term in the equation (4) and subsequently the boundary conditions can be introduced into the equation. The general finite element formulation which was derived by means of this approach can be finally written as

$$\left(K_d + K_k + K_\lambda + K_\alpha \right) C_i = q_\alpha + q_G \qquad (9).$$

The conductance matrix K_d is defined as

$$K_d = \int_{\Omega^{(e)}} D_e \left(\frac{\partial W_i}{\partial x} \frac{\partial N_i^{\,T}}{\partial x} + \frac{\partial W_i}{\partial y} \frac{\partial N_i^{\,T}}{\partial y} \right) \mathrm{d}\,\Omega ,$$

the convective transport matrix K_k as

$$K_k = \int_{\Omega^{(e)}} \frac{1}{\varepsilon} \left(u W_i \frac{\partial N_i^{\,T}}{\partial x} + v W_i \frac{\partial N_i^{\,T}}{\partial y} \right) \mathrm{d}\,\Omega ,$$

the radioactive decay matrix K_λ as

$$K_\lambda = \int_{\Omega^{(e)}} \lambda W_i N_i^{\,T} \mathrm{d}\Omega ,$$

the boundary conditions matrix K_α as

$$K_\alpha = \int_{\Gamma^{(e)}} \left(\alpha_c - \frac{v_n}{\varepsilon} \right) W_i N_i^{\,T} \, \mathrm{d}\,\Gamma$$

the boundary conditions vector q_α as

$$q_\alpha = \int_{\Gamma^{(e)}} \left(\alpha_c - \frac{v_n}{\varepsilon} \right) W_i \overline{C} \, \mathrm{d}\,\Gamma$$

and the radon generation rate vector q_G as

$$q_G = \int_{\Omega^{(e)}} G W_i \mathrm{d}\Omega .$$

Note that the convective transport matrix K_k is asymmetrical, which is caused by the fact that the differential operator in the equation (1) is not self-adjoint. This leads to the asymmetrical matrix of the linear equations system for unknown nodal values C_i.

The computer model „RADON“ developed by Z. Svoboda and M. Jiranek is based on the equations (3) and (9). It calculates the pressure field within the porous medium, the air flow velocity field, the radon concentration field and the radon exhalation rate due to diffusion and due to convection.

SIMULATION

The sub-slab soil ventilation system has been chosen as an example of simulation. The soil ventilation systems are designed to reduce soil gas flow from the ground into a building either by increasing or by decreasing the air pressure in the soil below a house. These systems may consist of a perforated pipe network beneath the building or of separate suction pits. The pressure difference is induced by means of a small fan or by means of a passive stack effect. The pressure difference should be extended under the entire area of the building in direct contact with the soil. The performance of soil ventilation systems is

dependent on the number of suction pits and their locations, on the number of perforated drain pipes and their diameters, on the distances between pipes and the pressure differential between the air in the building and the air in the pipes or suction pits.

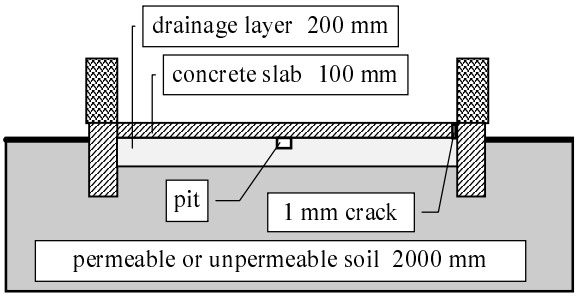

Fig. 1a Cross section of the theoretical model

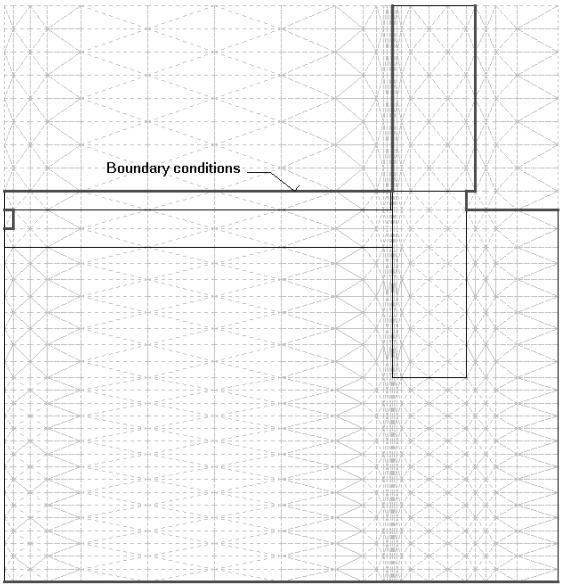

Fig. 1b Mesh system in part of the model

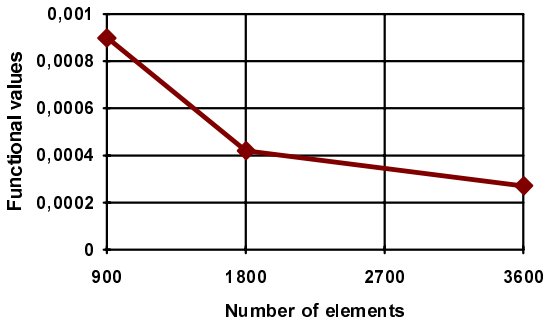

Fig. 1c The calculated functional values

Table 1 Used material characteristics

Material	Permeability [m^2]	Radon diffusion coefficient [$m^2.s^{-1}$]	Porosity [-]	Radon production rate [$Bq.m^{-3}s^{-1}$]
concrete (slab, footers)	1.10^{-17}	5.10^{-9}	0,05	0
masonry (walls)	1.10^{-14}	3.10^{-7}	0,25	0
gravel (drainage layer)	1.10^{-7}	1.10^{-4}	0,40	0
perme-able soil	1.10^{-11}	1.10^{-6}	0,30	0,2
unperme-able soil	1.10^{-16}	6.10^{-8}	0,50	0,2

The performance of one typical soil ventilation system has been studied on a theoretical model that represents a single family house without a basement. The cross section of the model is shown in Fig.1a.

The concrete slab is 5 m wide and 100 mm thick. It is placed between the footers and rests on a drainage layer of a highly permeable gravel, which releases no radon into the soil gas. Soil beneath the gravel is assumed to be either permeable or unpermeable with the radon production rate of 0,2 $Bq.m^{-3}s^{-1}$. All material characteristics used in this model are summarized in Table 1.

Radon concentration in the deep soil gas was assumed to be under the constant value of 100 $kBq.m^{-3}$ and in the house interior of 20 $Bq.m^{-3}$. Radon concentration in the outdoor air was set to 5 $Bq.m^{-3}$. The interior surface of the slab and brick walls was under a fixed depressurization of - 3 Pa.

The rectangular pit with a square cross section is placed at the centre of the model in the gravel immediately below the slab. The pressure difference imposed at this pit by means of the soil ventilation system was considered either 50 Pa (in case of the sub-slab pressurization system) or -50 Pa (in case of the sub-slab depressurization system). The pressure differences in the suction pits under the real houses usually vary from 30 to 200 Pa in dependence on the house geometry, on the soil and the drainage layer permeabilities and on the suction pits location.

The effect of the slab tightness on the operation of sub-slab ventilation system has been investigated by means of a crack of 1 mm width, located at the slab - wall joint.

This model was used to find out how the soil ventilation systems are influenced by the permeability of the soil, the permeability of the drainage layer, the

mode of soil ventilation (i.e. pressurization or depressurization), the slab tightness and the presence of the drainage layer.

Figure 1b shows the automatically generated mesh system in the right half of the model with total number of 3600 finite elements. This mesh system consisting of triangular finite elements was introduced into the calculation module of the program „RADON“. The numerical stability analysis was performed by means of the numerical evaluation of the functional corresponding to the equation (1). This functional has been calculated for the initial mesh system with 900 finite elements and then twice for the refined mesh system with the doubled number of finite elements. Figure 1c shows how the numerical value of the functional is influenced by the number of finite elements. It can be seen that the functional values decrease with increasing number of elements. As the exact solution of the equation (1) must minimize the corresponding functional, this dependence shows that the calculated results of the equation (1) converge to the exact solution with increasing number of elements.

The results of calculation obtained for the slab without cracks and for the slab with cracks show that the absence of the soil ventilation leads to a substantial increase in the radon entry rate caused by cracks in the slab. This effect has not been observed for houses on unpermeable soils with a great resistance to soil gas flow (see Fig. 2 and Fig. 3).

The effect of soil depressurization on the radon entry rate is not so significant if the concrete slab is tight (Fig. 2a and Fig. 3a). In case of permeable soil, the increased radon concentration in the vicinity of the suction pit (Fig. 4a) even leads to higher radon diffusion into the interior, but this transport is negligible. In case of unpermeable soil, the radon concentration field below the tight slab is not influenced by the depressurization. Reversed convective flow from the house into the soil is also insignificant.

Sub-slab pressurization systems applied to the permeable soils under the tight concrete slab ventilate the subsoil and thus dilute the radon concentration below the slab (Fig. 4a). Lower concentration causes a significant drop in the radon entry rate. In unpermeable soils the pressurization does not affect the radon concentration and the radon entry rate is not reduced. Convective flow from the soil into the house is negligible for both soil permeabilities.

Sub-slab depressurization systems inverting the pressure gradient across the slab are very effective for untight slabs with cracks. As a result of the pressure gradient inversion, the indoor air is sucked through cracks into the sub-slab region. This convective transport is directly proportional to the soil permeability. For that reason a drainage layer placed directly below the slab can very significantly improve the performance of the soil depressurization systems (compare Fig. 2b and Fig. 3b). If the drainage layer is placed above the unpermeable soil, depressurization systems dilute also the radon concentration below the slab (this is the only case when the soil depressurization can serve for the decreasing of radon concentration).

Soil pressurization systems are inconvenient for the houses with the untight slab. They are ineffective in soils with low permeability and in absence of the drainage layer (Fig. 4b). They even increase the radon entry rate in the presence of the drainage layer, mainly due to increased convective flow from the gravel into the house through the cracks in the concrete slab (Fig. 2b). The worst profile from this point of view is the drainage layer above the unpermeable soil.

Soil pressurization reduces radon concentration below the slab only in permeable soils (Fig. 4b) or in the presence of the drainage layer. Nevertheless, the low radon concentration does not automatically lead to the low radon entry rate, as was already explained above.

Several graphical outputs from the computer program are documented in Fig. 5 and Fig. 6. These figures show the pressure fields and the radon concentration fields beneath the slab in dependence on soil permeability, presence of drainage layer and mode of soil ventilation. They also demonstrate that the drainage layer plays a crucial role in ensuring of the pressure field extension throughout the sub-slab region. Figures correspond with the above mentioned results. They clearly show the drop in radon concentration below the slab due to pressurization of permeable soils and the increase of radon concentration below the slab caused by depressurization of the soil with high permeability.

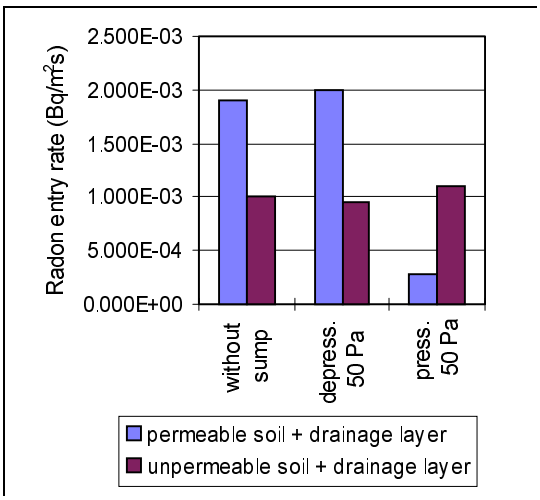

Fig. 2a Radon entry rate in case of tight concrete slab and drainage layer

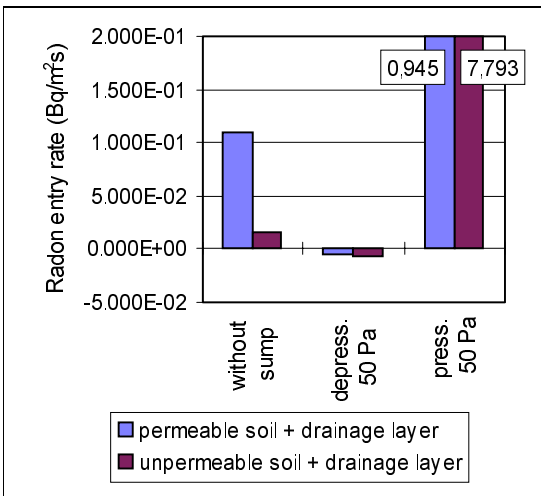

Fig. 2b Radon entry rate in case of untight concrete slab and drainage layer

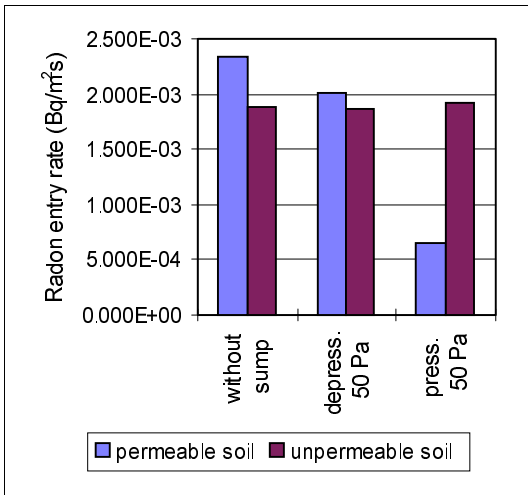

Fig. 3a Radon entry rate in case of tight concrete slab and no drainage layer

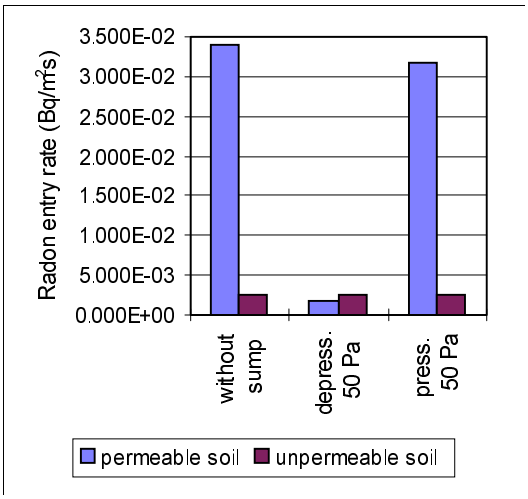

Fig. 3b Radon entry rate in case of untight concrete slab and no drainage layer

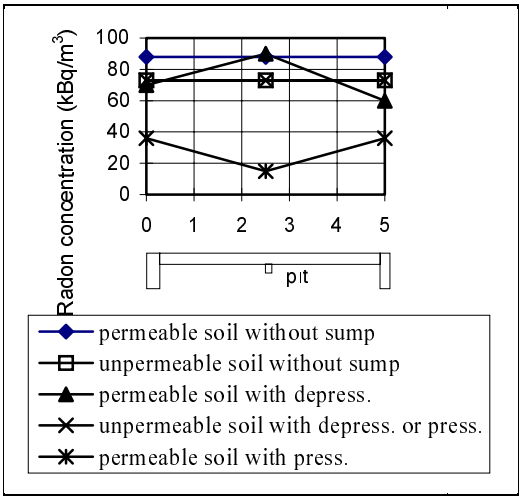

Fig. 4a Radon concentration in the soil immediately beneath the tight concrete slab

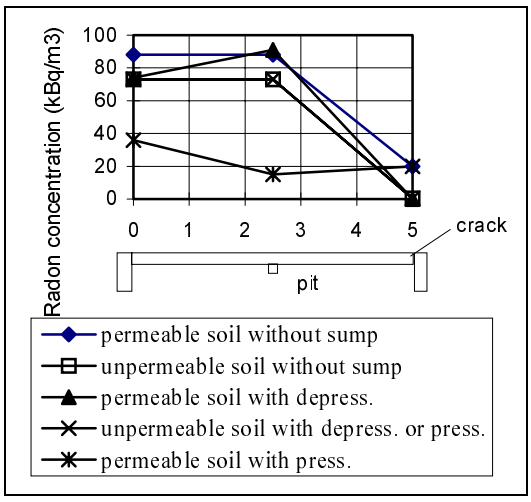

Fig. 4b Radon concentration in the soil immediately beneath the untight concrete slab

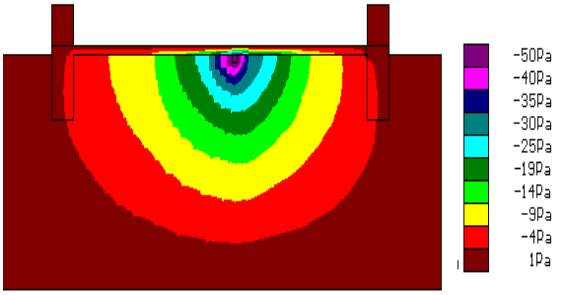

Fig. 5a Results for soil depressurization system (- 50 Pa) in the permeable soil under slab with crack and no drainage layer - the pressure field

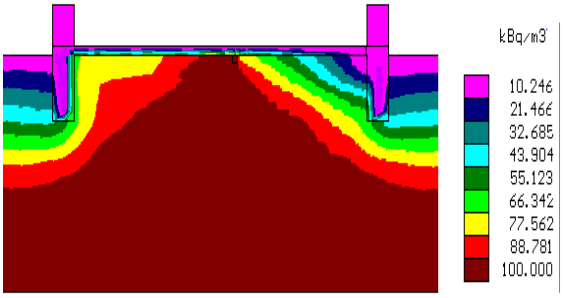

Fig. 5b Results for soil depressurization system (- 50 Pa) in the permeable soil under slab with crack and no drainage layer - the radon concentration field

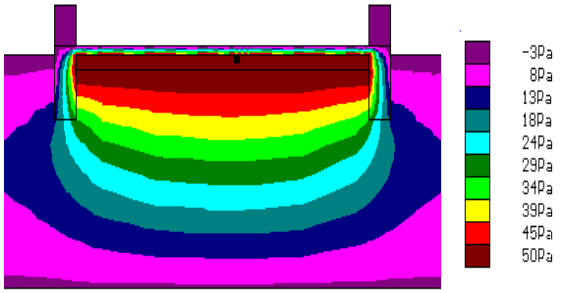

Fig. 6a Results for soil pressurization system (+ 50 Pa) in the permeable soil under slab with drainage layer and no crack - the pressure field

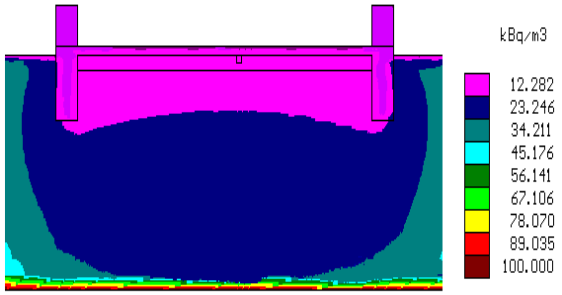

Fig. 6b Results for soil pressurization system (+ 50 Pa) in the permeable soil under slab with drainage layer and no crack - the radon concentration field

CONCLUSIONS

The computer model „RADON“ could be used for simulation of various radon protective measures. This work presents its application as a verification tool for the soil ventilation systems.

The results of the numerical modeling of the soil ventilation systems show these major conclusions:

- Pressure field extension below the slab is substantially dependent on the soil permeability or on the presence of the drainage layer. The higher the permeability, the better the extension.
- Soil depressurization systems are suitable for the majority of cases - even for untight slabs. Their performance can be significantly improved by the drainage layer.
- Soil pressurization systems can be successfully applied only to the permeable soils. They are not convenient for untight slabs. Drainage layer above low permeable soils even considerably increases the radon entry rate into the building.

REFERENCES

Zienkiewicz, O.C., Taylor, R.L., „The Finite Element Method, Fourth edition“, McGraw-Hill, 1991.

Huebner, K.H., Thornton, E.A., „The Finite Element Method for Engineers, Second edition“, J. Wiley & Sons, 1982.

Jiránek, M., „Modelling the Behaviour of Soil Ventilation Systems“, In: Radon Investigations in the Czech Republic VI, pp. 136 - 140, Praha 1996.

NOMENCLATURE

C	radon concentration in the soil gas [Bq.m^{-3}]
C_i	vector of unknown radon concentration values
$\overline{C}$	radon concentration at the element boundary
D_e	effective radon diffusion coefficient [m^2.s^{-1}]
G	radon generation rate [Bq.m^{-3}.s^{-1}]
h	size of an element in the velocity direction
k	permeability of the porous medium [m^2]
K_d	conductance matrix
K_k	convective transport matrix
K_λ	radioactive decay matrix
K_α	boundary conditions matrix

N_i	interpolation functions vector
p	pressure of the soil gas [Pa]
Pe	Peclet number
q_α	boundary conditions vector
q_G	radon generation rate vector
$\|u\|$	velocity vector magnitude
u	velocity component in the x axis direction
$\vec{v}$	velocity vector of soil gas flow [$m.s^{-1}$]
v	velocity component in the y axis direction
v_n	velocity component normal to the boundary
W_i	weighting functions vector
α_c	radon transfer coefficient [$2,0.10^{-3}$ $m^2.s^{-1}$]
ε	porosity of the porous medium [-]
Γ_e	boundary of a finite element
η	dynamic viscosity of the soil gas [Pa.s]
λ	radon decay constant [$2,1.10^{-6}$ s^{-1}]
Ω_e	area of a finite element